

Adsorption of Carbendazim Pesticide on Plasmonic Nanoparticles Studied by Surface- Enhanced Raman Scattering

L.N. Furini^a, C. J. L. Constantino^a, S. Sanchez-Cortes,^b J.C. Otero,^c I. López-
Tocón^{c,*}

^aFCT, Universidad Estadual Paulista, Presidente Prudente, SP, Brazil.

^bInstituto de Estructura de la Materia, CSIC, Serrano 121, E-28006-Madrid,
Spain.

^cDepartment of Physical Chemistry, Faculty of Science, University of Málaga,
Unidad Asociada CSIC, E-29071-Málaga, Spain.

*Corresponding author: I. López-Tocón, e-mail: tocon@uma.es

Abstract

Surface-enhanced Raman spectra (SERS) of methyl N-(1H-benzimidazol-2-yl)carbamate (MBC), usually named carbendazim, have been recorded on silver colloids at different pH values. In order to identify the neutral, protonated or deprotonated species of MBC that originate the SERS, the vibrational wavenumbers of these three isolated forms and linked to a silver atom have been predicted by carrying out DFT calculations. The results indicate that the active SERS species in the studied pH range correspond to the neutral MBC and its deprotonated ion in the amidate form. According to theoretical calculations, neutral MBC is linked to the metal through the imidazolic nitrogen atom, while the deprotonated MBC could be linked through the imidazolic nitrogen together with the amidic nitrogen atom or the carbonyl oxygen atom. Both adsorbed species, neutral and deprotonated, have the benzimidazolic ring orientated almost perpendicular to the silver surface and no molecular reorientation has been detected. The relative abundance of the neutral MBC and its amidate anion is experimentally followed through the intensities of the SERS bands recorded at about 1230 and 1270 cm^{-1} . These two key lines correspond to the in-plane NH deformation of amidic and imidazolic groups, respectively, which can be used as pH sensor.

Introduction

Benzimidazole derivatives are heterocyclic compounds of great interest for their technological, medical and biological application as inhibitors of some corrosion processes,¹ chelating agent to bind metals in case of metal poisoning,² or antiparasitics to control helminthes species which attack humans and animals.³ However, they are used primarily as fungicides and pesticides of broad-spectrum efficacy to control fungal diseases in fruits and vegetables.⁴ Despite the usefulness of these compounds, some of them are classified as pollutants by European Union establishing their concentration limit in different samples. This is the case of methyl N-(1H-benzimidazol-2-yl)carbamate (MBC), usually named carbendazim, which is a benzimidazole derivative where the imidazolic hydrogen atom is substituted by a carbamate group. MBC is a systemic fungicide, white powder, with very low solubility in water ~ 6.11 mg/L. It has two pK_a ($pK_{a1}=4.5$ and $pK_{a2}=10.6$) controlling the relative abundance of protonated (MBC^+), neutral (MBC^0) and deprotonated (MBC^-) forms in aqueous solution, depending on the pH (Figure 1).⁵

Although several analytical methods have been proposed to identify and quantify the presence of environmental pollutants,^{6,7} new spectroscopic techniques like Surface-Enhanced Raman Scattering (SERS) do not require pre-treatment of the sample for a routine control.^{8,9} SERS is nowadays used for sensitive and selective molecular identification due to the giant electromagnetic (EM) enhancement of the Raman signal induced by localized plasmon resonances in nanostructured noble metal surfaces.^{10,11} This huge enhancement provide strong Raman signals from very insoluble compounds such as MBC⁵ and allows, for instance, to record the spectra of hydrophobic molecules in aqueous solution at trace level by using molecular hosts of specific analytes such as viologen dications^{9,12} or cyclodextrins¹³ among others.

Beside analytical applications as chemical sensor, SERS is also a powerful tool to gain insight into the nature of the metal-adsorbate hybrid, the bonded molecular species and its chemical interaction with the metal nanostructure.¹⁴⁻¹⁶ SERS spectra of simple molecules related to MBC such as benzimidazole (BIZ)¹⁶ and imidazole (IZ)¹⁵ have been previously studied. In the case of BIZ two different types of adsorption are proposed depending on the pH, through the π -electrons of the aromatic ring at neutral pH or through the lone pair of the nitrogen atom at acidic pH, as occurs in heterocyclic molecules like diazines¹⁷ and IZ.¹⁶ A similar behavior was found in the case of cyanide ion where a molecular reorientation from perpendicular to parallel adsorption occurs when the cyanide concentration is lowered.¹⁸

MBC is a much more complex adsorbate given that three different chemical species have to be considered depending on the pH: the neutral molecule (MBC^0) and the protonated (MBC^+) and the deprotonated (MBC^-) charged species. The energies of both ionic forms are stabilized by resonance because of the positive or negative charge can be delocalized along the aromatic heterocyclic ring and the carbamate group. This effect slightly increases the basicity of the imidazolic nitrogen ($\text{pK}_{\text{a}1}=4.5$) with respect to other compounds with sp^2 hybridization¹⁹ although remains less basic than the imidazole ($\text{pK}_{\text{a}}=7.0$), the aliphatic amines ($\text{pK}_{\text{a}}=10-11$) and ammonia ($\text{pK}_{\text{a}}=9.24$). On the other hand, the amidic nitrogen atom located in the carbamate group is slightly more acid ($\text{pK}_{\text{a}2}=10.6$) than the aliphatic amides ($\text{pK}_{\text{a}}=14-15$).¹⁹

This work is mainly focused on the study of the effect of the pH in the coordination of a complex molecular system like MBC on metallic plasmonic surfaces by means of SERS in order to identify the adsorbed species and the specific interacting center with the metal. In this way, SERS spectra of 10^{-5} mol/L MBC have been recorded on silver sols at several pH values ranging from pH=2 up to 12. The analysis of the

results has been carried out with the help of Density Functional Theory (DFT) calculations which have proved once again their usefulness in the spectral interpretation.

Methods

All reagents and MBC were purchased from Sigma-Aldrich. Stock solutions (10^{-3} mol/L) of MBC were prepared with ethanol (100%) provided by VWR, Prolab. Silver sols and aqueous solutions were prepared with water from Milli-Q system (18.2 M Ω .cm resistivity).

Preparation of Ag nanoparticles and SERS measurements. Ag nanoparticles (AgNPs) were prepared by reducing an aqueous solution of silver nitrate (10^{-2} mol/L) with hydroxylamine hydrochloride (1.66×10^{-3} mol/L) in alkaline medium (300 μ L NaOH 1.0 mol/L) under vigorous stirring according to the procedure described elsewhere.^{20,21} Other reducing agents such as citrate and NaBH₄ can be alternatively used to obtain colloidal suspensions, but it has been shown that the NPs obtained by using hydroxylamine show a more uniform distribution of size and shape and no interferences from the remaining oxidation products are detected.²² AgNPs were characterized by the resonances of metallic plasmons in the UV-VIS spectra, showing a maximum at about 410 nm with an average FWHM of 80 nm.

AgNPs colloids were previously activated by adding 40 μ L KNO₃ (0.5 mol/L) to 960 μ L of AgNPs in a 1cm x 1cm cuvette. The final pH of the mixture was adjusted to 2, 6, 8, 10 and 12 by adding HNO₃ or NaOH. The aggregation induced by KNO₃ leads to a slight change of the color as well as an enhancement of the plasmon adsorption at higher wavelengths. Then, an aliquot of 10 μ L was removed from the mixture and 10 μ L of MBC solution was added in order to keep the volume in 1000 μ L. The final MBC concentration was 10^{-5} mol/L in all the pH range.

Raman spectra were obtained using a micro-Raman inVia Renishaw spectrograph, equipped with an electrically cooled CCD camera, under 532 nm excitation and diffraction grating of 1800 1/mm. The laser power reaching the sample was about 2.0 mW and the spectral resolution was set to 2 cm^{-1} . Raman spectrum of powder was recorded using the 785 nm exciting line to avoid fluorescence emission. The UV-VIS extinction spectra of aggregated colloid suspensions of MBC diluted to 10% in water have been recorded in a Cintra 5 spectrophotometer using an 1 cm pathlength cell.

Theoretical calculations. Optimized structure and force field of neutral MBC^0 , BIZ and IZ were calculated at B3LYP/6-31G* level of theory. It has been demonstrated that this level of calculation reproduces satisfactorily the vibrational spectrum of aromatic molecules.^{23,24} Geometry optimization of MBC^0 has been constrained to a planar structure (Cs symmetry) where an intramolecular hydrogen bond occurs between the imidazolic NH bond and the amidic oxygen atom. This MBC^0 structure agrees with the local symmetry in solid phase, providing a higher crystallinity than BIZ²⁵ and a lower solubility in water as well as a higher melting point of MBC in comparison to BIZ.¹³ The optimized structure of protonated and deprotonated MBC, (MBC^+ and MBC^- , respectively) and their corresponding vibrational wavenumbers have also been calculated. Figure 1 shows the B3LYP/6-31G* optimized geometry of the MBC species and summarizes the nomenclature used for the two different NH bonds: imidazolic NH_{IZ} and amidic NH_{AM} .

In addition, a simple molecular model has been assumed for the MBC-Ag surface complex involving a single silver atom linked to the three different chemical species of MBC (Figure 2). A positive or negative silver atom has been selected depending of the negatively/neutral or positively charged MBC forms, respectively, in order to minimize the electrostatic repulsion between the AgNP and the adsorbate

because of larger SERS enhancement is detected under this condition.²⁶ B3LYP method with the LanL2DZ basis set has been employed for calculating the respective optimized structures and force fields of the different complexes ($\text{MBC}^0\text{-Ag}^+$, $\text{MBC}^+\text{-Ag}^-$, $\text{MBC}^-\text{-Ag}^+$). This is the same level of calculation previously used by us for analyzing the adsorption and charge transfer processes in the SERS of benzene-like molecules.^{27,28} The silver cation is bonded to the imidazolic or the amidic nitrogen atoms in the optimized complexes of MBC^0 or MBC^- species, respectively, as occurs in heterocyclic aromatic molecules where the nitrogen atom is preferred to adsorb on the metallic surface.^{29,30} In the case of MBC^+ , the only possible interaction with silver is through the π -system of the aromatic rings given that all the nitrogen are bonded to hydrogen. As expected, the $\text{MBC}^+\text{-Ag}^+$ complex dissociates in the optimization process. Therefore, a negatively charged silver atom has been considered in order to predict the vibrational wavenumbers associated to this species ($\text{MBC}^+\text{-Ag}^-$). All the calculated wavenumbers of the different complexes are real indicating that the optimized geometries correspond to equilibrium structures and no scaling factor was used for the force field given that the accuracy of B3LYP vibrational wavenumbers are typically better than 95% of the experimental values.³¹ All calculations have been carried out using the GAUSSIAN09 program package.³²

Results and discussion

SERS spectra of carbendazim at different pH. Raman spectrum of solid MBC (Figure S1) has been recorded giving that the low solubility of MBC prevents recording the Raman from aqueous solutions at any pH value. This spectrum is dominated by seven strong bands recorded at 1475, 1271, 1262, 1030, 961, 724 and 618 cm^{-1} as well as two very strong bands at lower wavenumbers ($<150\text{ cm}^{-1}$) which correspond to lattice

vibrations. The remaining bands recorded in the 200-1800 cm^{-1} region show a much lower intensity than the previous ones. Table S1 shows the vibrational assignment of MBC taking into account the B3LYP/6-31G* force field of the isolated chemical species and the reported assignment³³⁻³⁸ of related molecules. The bands associated to the amidic and imidazolic NH bonds have been highlighted, it being very interesting the 1200-1300 cm^{-1} region in order to recognize the presence of a particular ionized form of MBC given that characteristic bands of specific deprotonated species are recorded at these wavenumbers.

Figures 3 and 4 show the medium and high wavenumber regions, respectively, of SERS spectra of MBC recorded at different pH values. All the spectra have been normalized to the corresponding strongest band, except for the weak SERS at pH=2 which shows a very strong background. SERS at pH=6 is almost identical to that at pH=8 and both spectra are dominated by five strong SERS bands recorded at about 1520, 1460, 1270, 1230 and 1010 cm^{-1} . However, in the SERS at pH=10 the relative intensities of the doublets appearing at 1230/1270 cm^{-1} (Figure 3) and 2950/3070 cm^{-1} (Figure 4) are reversed. As a consequence, the bands at 1270 and 2950 cm^{-1} become the strongest ones of the respective pairs when the pH is basic enough. The dependence of the relative intensities of these bands on the pH can be related to the normal modes of the functional groups which undergo deprotonation, i.e. the amidic and imidazolic NH groups, and therefore, these bands can be used to recognize the adsorption of the three possible ionized species on the basis of the force field calculations.

Vibrational assignment of MBC. The analysis of the vibrational and SERS spectra of a complex molecular system such as MBC has been carried out on the basis of the force field calculations and the assignments of BIZ^{16,33} and IZ^{15,34-36} related molecules. Table S1 correlates the experimental Raman wavenumbers of solid MBC

and those of BIZ and IZ together with those calculated by using the B3LYP/6-31G* method for all the considered chemical species. Table S2 summarizes in turn the wavenumbers of MBC recorded at different pH values and the B3LYP/LanL2DZ theoretical ones for the different MBC-Ag surface complexes.

The strongest SERS bands (Figure 3) are assigned to in-plane normal modes and only few lines correspond to out-of-plane fundamentals. The five strong SERS bands recorded at about 1520, 1460, 1270, 1230 and 1010 cm^{-1} at $\text{pH} \geq 6$ are assigned to vibrational motions involving $\delta\text{NH}_{\text{AM}}$, $\delta\text{NH}_{\text{AM}}+\delta\text{CH}_3$, $\delta\text{NH}_{\text{IZ}}$, $\delta\text{NH}_{\text{AM}}$ and $\delta\text{CC}_{\text{Bz}}$ in-plane deformations, respectively. The characteristic vibrational modes of the amide group have also been identified. Amide I vibration, recorded at about 1650 cm^{-1} , arises mainly from the C=O stretching coordinate and the Amide II band, recorded at about 1550 cm^{-1} , corresponds to a combination of the NH_{AM} in-plane bending and the CN stretching coordinates. Although this last band is usually weak or absent in the Raman spectrum of polypeptides, the medium-strong SERS band observed at 1520 cm^{-1} can be assigned to Amide II. This band splits in two components at $\text{pH}=10$, 1520 and 1507 cm^{-1} , being that recorded at 1520 cm^{-1} slightly weaker than the new one at 1507 cm^{-1} and, finally, becomes very weak appearing as a shoulder at $\text{pH}=12$. The force field predicts one or two fundamentals in this region, depending of the considered MBC^- or MBC^0 species, at 1528 and 1542 cm^{-1} and assigned to NH_{IZ} and NH_{AM} in-plane deformations, respectively, (Table S1). The Amide III vibration of MBC, recorded with strong intensity at 1230 cm^{-1} , corresponds to a combination of NH_{AM} bending and CC benzenic stretching coordinates. Another strong SERS band is appearing at 1270 cm^{-1} which contains a large contribution from NH_{IZ} in-plane deformation.

There are also a couple of bands recorded over 1400 cm^{-1} showing a similar behavior to that described for the 1200 and 1500 cm^{-1} regions, that is, their relative

intensities are reversed at basic pH in agreement with the proposed assignment giving that both fundamentals are related to the NH_{AM} and NH_{IZ} in-plane deformations.

Regarding the high wavenumber region (Figure 4), two broad SERS bands are recorded in all spectra at about 3400 and 3200 cm^{-1} , respectively. Their intensities are not depending on pH and are due to water. However, two bands appear at lower wavenumber, 3070 and 2950 cm^{-1} , whose relative intensities are very sensitive to the pH and are reversed like occurs with the key bands recorded at 1230 and 1270 cm^{-1} . This implies that they should be also related to the amidic and imidazolic NH groups. These bands are involved in a Fermi resonance^{37,38} concerning the CH stretching modes of aromatic molecules,³³ recorded at about 3000 cm^{-1} , and the overtone of the strong fundamentals at 1500 cm^{-1} assigned to the amidic and imidazolic in-plane NH deformation as explained. Accordingly, the bands at 3070 and 2950 cm^{-1} have been assigned to the mentioned combination of aromatic CH stretching and the overtone of the NH amidic and imidazolic deformations, respectively.³⁹

Adsorption of MBC on Ag nanoparticles. The analysis of the B3LYP/LanL2DZ calculated wavenumbers of the three different Ag-MBC surface complexes ($\text{MBC}^0\text{-Ag}^+$, $\text{MBC}^-\text{-Ag}^+$, $\text{MBC}^+\text{-Ag}^-$, Figure 2 and Table S2) indicates that the main changes should correspond to the fundamentals related to the ionizable imidazolic and amidic groups. Generally speaking, the interaction of the imidazole ring with the surface seems to dominate the adsorption of MBC on silver, even in the case of neutral MBC^0 , as pointed out by the calculated fundamentals at 1027 and 1363 cm^{-1} of the complex with Ag^+ .

In addition, most of the enhanced bands in the SERS spectrum, such as those recorded at ca. 1520, 1270, 1230 and 1010 cm^{-1} , correspond to in-plane normal modes what suggests a perpendicular orientation of the molecule with respect to the metallic

surface on the basis of the propensity rules of the EM enhancement mechanism of SERS.⁴⁰

The chemical species adsorbed on the silver surface can be checked by analyzing the dependence on the pH of the relative SERS intensities of the pairs of the bands assigned to amidic/imidazolic groups. The most striking feature is the behavior of the bands recorded at 1230/1270 cm^{-1} and assigned to NH_{AM} and NH_{IZ} in-plane deformations, respectively, where the relative intensity of the 1230 cm^{-1} line decreases when pH increases. There are also other bands sensitive to the pH recorded in the 1300 and 1400 cm^{-1} region as, for instance, the bands assigned to the amidic group (1340 and 1460 cm^{-1}) that become weaker than the assigned to imidazolic group (1380 and 1430 cm^{-1}) when the pH is raised. The same occurs in the 1500 cm^{-1} region. The band recorded at 1522 cm^{-1} (amidic group) shows a shoulder at 1505 cm^{-1} (imidazolic group) in the SERS at pH=10 and dominates at pH=12. These results indicate that the MBC^0 and MBC^- chemical species are adsorbed on the nanoparticles and that the MBC^+ species is not able to interact with the surface. The imidazolic N atom is involved in the adsorption process and only when MBC^0 species is present in the sol (pH>6) an enhancement of SERS intensity is observed. This is also observed in the VIS spectra of MBC colloidal solutions measured at different pH (Figure 5). A new band at high wavelength (≈ 780 nm), and characteristic of aggregation, appears in the spectra at pH>6, indicating that the adsorption of MBC on AgNPs is only effective when the pesticide is in neutral or anionic forms, thus corroborating that the IZ group is involved in the interaction with the metal. These evidences, together with the absence of any SERS band recorded at ca. 1295 cm^{-1} which is assigned to NH deformation of the protonated imidazolic nitrogen (see Table S2), corroborates that MBC^0 or MBC^- species originate the SERS.

This conclusion is further supported by the attempts to calculate the optimized B3LYP/LanL2DZ geometry of the MBC^+-Ag^+ . These calculations do not converge to any minimum given that the MBC^+ cation does not have any free nitrogen atom able to interact with the metallic surface. Only an optimized geometry for the MBC^+-Ag^- complex has been obtained where the negatively charged silver atom is located above the aromatic ring (see Figure 2a). In this case, the MBC^+ loses the planarity because of the imidazolic carbon pyramidalizes while the silver anion is located above the three nitrogen atoms. This kind of interaction would give rise to the enhancement of SERS bands corresponding to the out-of-plane normal modes⁴⁰ but no bands assigned to these vibrations are enhanced what discards the adsorption of the cationic MBC^+ species.

Therefore, MBC^0 and its amidate anion MBC^- are the two chemical species adsorbed on the metallic surface. The optimized structure of the MBC^0-Ag^+ complex yields a planar geometry with Cs symmetry, where the silver atom is bonded to the imidazolic nitrogen atom giving a perpendicular orientation of the adsorbate with respect to the metallic surface (Figure 2b). The calculated vibrational wavenumbers for this complex are in agreement with the experimental ones. The MBC^- species contains the amidate group and can be adsorbed through either both the imidazolic and the amidic nitrogen atoms (N-Ag-N), or the imidazolic nitrogen and the carbonyl oxygen atom (N-Ag-O) as show the corresponding optimized structures (Figure 2c). The calculated force fields for both metallic complexes predict very similar wavenumbers in agreement with the experimental results and the energy difference between these two structures is very small (1.2 Kcal/mol), being the last complex slightly more stable.

In addition, the relative intensity of the pair of bands recorded at 1230/1270 cm^{-1} can be used as a sensor of pH given that it is related to the relative abundance of $\text{MBC}^0/\text{MBC}^-$ species. A linear dependence can be appreciated in Figure 6 where the relative intensity of these bands is plotted vs. pH. A similar dependence is obtained if

the respective intensities of these two bands are plotted vs. that recorded at, for instance, 626 or 1006 cm^{-1} . In the case of the band at 1230 cm^{-1} it is possible to establish a direct relationship between the ionization state of the adsorbate and the pH because the ionizable NH_{AM} bond is not involved in the adsorption as occurs in para-mercaptobenzoic acid.⁴¹ On the contrary, simple carboxylic acids or amides are no valid pH SERS-sensors because the ionizable chemical group is also involved in the linkage with the metal.⁴²

Conclusions.

The identification of the chemical species of MBC adsorbed on Ag nanoparticles has been carried out by analyzing the dependence of the SERS spectra on the pH on the basis of DFT quantum mechanical calculations. A complete vibrational assignment of all the possible chemical species adsorbed on the silver surface has been proposed. The SERS active forms correspond to the neutral MBC and its amidate ion (MCB^-) with perpendicular orientation with respect to the metallic surface, given that no out-of-plane bands are enhanced in SERS. The changes in the intensities of the pairs or SERS bands recorded in the 1200 cm^{-1} and 3000 cm^{-1} regions when the pH is raised evidence the of the relative concentration of neutral/amidate species. Moreover, the theoretical results point out to a change of the MBC coordination to Ag surface which goes from monodentate at neutral pH (through the imidazolic nitrogen atom of neutral MBC) to bidentate at basic pH (through both imidazolic and amidic nitrogen atoms or the oxygen atom of the amidate group). Finally a linear dependence between the relative intensity of the 1230/1270 cm^{-1} bands on the pH has been found because of the amide group is not involved in the adsorption. This allows for using this molecule as pH-sensor by using SERS spectroscopy in the 4-14 pH range.

Acknowledgment

We are grateful to the Spanish MINECO (CTQ2012-31846, FIS2010-15405) and Junta de Andalucía (FQM-5156 and 6778), and to the Brazilian agencies CAPES, CNPq and FAPESP, for financial support. The authors thank to SCAI and Rafael Larrosa (UMA) for computational facilities.

Supporting Information Available: Figure S1 showing the Raman spectrum of solid MBC and Tables S1 and S2 summarizing the experimental (Raman and SERS) and theoretical DFT vibrational wavenumbers of BIZ, IZ and MBC and of different silver complexes. This material is available free of charge via the Internet at <http://pubs.acs.org>.

References

- (1) Xue, G.; Lu, Y.; Shi, G. *Appl. Surf. Sci.* **1994**, *74*, 37-41.
- (2) Barker, H.A.; Smyth, R.D.; Weissbach, H.; Toohey, J.I.; Ladd, J.N.; Volcani, B.E. *J. Biol. Chem.* **1960**, *235*, 480-488.
- (3) Lezcano, M.; Al-Soufi, W.; Novo, M.; Rodríguez-Núñez, E.; Tato, J.V. *J. Agric. Food Chem.* **2002**, *50*, 108-112.
- (4) Zhu, H.S.; Wu, L.H.; Li, R.B.; Xia, L.A.; Han, J.Q.; Zhang, Q.J.; Bian, Y.C.; Yu, Q.R. *Anal. Chim. Acta* **2008**, *619*, 165-172.
- (5) Ni, N.; Sanghvi, T.; Yalkowsky, S.H. *Int. J. Pharm.* **2002**, *244*, 99-104.
- (6) Pozo, M.; Hernández, L.; Quintana, C. *Talanta* **2010**, *81*, 1542-1546.
- (7) Vo-Dinh, T.; Fetzer, J.; Campliglia, A. D. *Talanta* **1998**, *47*, 943-969.
- (8) Garrell, R.L. *Anal. Chem.* **1989**, *61*, 401-411.
- (9) López-Tocón, I.; Otero, J.C.; Arenas, J.F.; Garcia-Ramos, J.V.; Sanchez-Cortes, S. *Anal. Chem.* **2011**, *83*, 2518-2525.
- (10) Moskovits, M. *Rev. Mod. Phys.* **1985**, *57*, 783-826.
- (11) Aroca, R. *Surface-Enhanced Vibrational Spectroscopy*; John Wiley & Sons, Chichester, U.K. **2006**.
- (12) Guerrini, L.; Garcia-Ramos, J.V.; Domingo, C.; Sanchez-Cortes, S. *Anal. Chem.*, **2009**, *81*, 1418-1425.
- (13) Leyton, P.; Sánchez-Cortes, S.; Garcia-Ramos, J.V.; Domingo, C.; Campos-Vallette, M.; Saitz, C.; Clavijo, R.E. *J. Phys. Chem. B*, **2004**, *108*, 17484-17490.
- (14) Ojha, A.K. *Chem. Phys.* **2007**, *340*, 69-78.
- (15) Loo, B.H.; Tse, Y.; Parsons, K.; Adelman, C.; El-Hage, A.; Lee, Y.G. *J. Raman Spectrosc.* **2006**, *37*, 299-304.

- (16) Kim, M.S.; Kim, M.K.; Lee, C.J.; Jung, Y.M.; Lee, M.S. *Bull. Korean Chem. Soc.* **2009**, *30*, 2930-2934.
- (17) Muniz-Miranda, M.; Neto, N.; Sbrana, G. *J. Phys. Chem.* **1988**, *92*, 954-959.
- (18) Kellogg, D.S.; Pemberton, J.E. *J. Phys. Chem.* **1987**, *91*, 1120-1126.
- (19) Streitwieser, A.; Heathcock, C.H.; Kosower, E.M. *Introduction to Organic Chemistry*; Prentice-Hall, **1998**.
- (20) Guerrini, L.; Garcia-Ramos, J.V.; Domingo, C.; Sanchez-Cortes, S. *Anal. Chem.* **2009**, *81*, 953-960.
- (21) Leopold, N.; Lendl, B. *J. Phys. Chem. B* **2003**, *107*, 5723-5727.
- (22) Cañamares, M.V.; Garcia-Ramos, J.V.; Gómez-Varga, J.D.; Domingo, C.; Sanchez-Cortes, S. *Langmuir* **2005**, *21*, 8546-8553.
- (23) Bencivenni, L.; Ramondo, F.; Pieretti, V.; Sanna, N. *J. Chem. Soc. Perkin Trans. 2*, **2000**, 1685-1693.
- (24) Giffin, G.A.; Boesch, S.; Bopege, D.N.; Powell, D.R.; Wheeler, R.A.; Frech, R. *J. Phys. Chem. B* **2009**, *113*, 15914-15920.
- (25) Dik-Edixhoven, C.J.; Schent, H.; Van der Meer, H. *Cryst. Struct. Commun.* **1973**, *2*, 23-24.
- (26) Alvarez-Puebla, R.A.; Arceo, E.; Goulet, P.J.G.; Garrido, J.J.; Aroca, R.F. *J. Phys. Chem. B* **2005**, *109*, 3787-3792.
- (27) Centeno, S.P.; López-Tocón, I.; Roman-Perez, J.; Arenas, J.F.; Soto, J.; Otero, J.C. *J. Phys. Chem. C* **2012**, *116*, 23639-23645.
- (28) Avila, F.; Fernandez, D.J.; Arenas, J.F.; Otero, J.C.; Soto, J. *Chem. Commun.* **2011**, *47*, 4210-4212.
- (29) Soto, J.; Fernández, D.J.; Centeno, S.P.; López Tocón, I.; Otero, J. C. *Langmuir* **2002**, *18*, 3100-3104.

- (30) Sardo, M.; Ruano, C.; Castro, J.L.; López-Tocón, I.; Soto, J.; Ribeiro-Claro, P.; Otero, J.C. *Phys. Chem. Chem. Phys.* **2009**, *11*, 7437-7443.
- (31) Cai, Z.Q.; Zhu, Y.X.; Zhang, Y. *Spectrochim. Acta, Part A* **2008**, *69*, 130-133.
- (32) Gaussian 09, Revision **D.01**, Frisch, M. J.; Trucks, G. W.; Schlegel, H. B.; Scuseria, G. E.; Robb, M. A.; Cheeseman, J. R.; Scalmani, G.; Barone, V.; Mennucci, B.; Petersson, G. A.; Nakatsuji, H.; Caricato, M.; Li, X.; Hratchian, H. P.; Izmaylov, A. F.; Bloino, J.; Zheng, G.; Sonnenberg, J. L.; Hada, M.; Ehara, M.; Toyota, K.; Fukuda, R.; Hasegawa, J.; Ishida, M.; Nakajima, T.; Honda, Y.; Kitao, O.; Nakai, H.; Vreven, T.; Montgomery, J. A., Jr.; Peralta, J. E.; Ogliaro, F.; Bearpark, M.; Heyd, J. J.; Brothers, E.; Kudin, K. N.; Staroverov, V. N.; Kobayashi, R.; Normand, J.; Raghavachari, K.; Rendell, A.; Burant, J. C.; Iyengar, S. S.; Tomasi, J.; Cossi, M.; Rega, N.; Millam, M. J.; Klene, M.; Knox, J. E.; Cross, J. B.; Bakken, V.; Adamo, C.; Jaramillo, J.; Gomperts, R.; Stratmann, R. E.; Yazyev, O.; Austin, A. J.; Cammi, R.; Pomelli, C.; Ochterski, J. W.; Martin, R. L.; Morokuma, K.; Zakrzewski, V. G.; Voth, G. A.; Salvador, P.; Dannenberg, J. J.; Dapprich, S.; Daniels, A. D.; Farkas, Ö.; Foresman, J. B.; Ortiz, J. V.; Cioslowski, J.; Fox, D. J. Gaussian, Inc., Wallingford CT, 2009.
- (33) Morsy, M.A.; Al-Khaldi, M.A.; Suwaiyan, A. *J. Phys. Chem. A* **2002**, *106*, 9196-9203.
- (34) Yoshida, C.M.; freedman, T.B.; Loehr, T.M. *J. Am. Chem. Soc.* **1975**, *97*, 1028-1032.
- (35) Carter, D.A.; Pemberton, J.E. *Langmuir* **1992**, *8*, 1218-1225.
- (36) Majoube, M.; Henry, M.; Chinsky, L.; Turpin, P.Y. *Chem. Phys.* **1993**, *169*, 231-241.
- (37) Krimm, S.; Bandekar, J. *Adv. Protein Chem.* **1986**, *38*, 181-364.
- (38) Barth, A.; Zscherp, C. *Quart. Rev. Biophys* **2002**, *35*, 369-430.

- (39) Bellanato, J. *J. Spectrochim. Acta* **1960**, *16*, 1344-1357.
- (40) Moskovits, M.; DiLella, D.P.; Maynard, K.J. *Langmuir* **1988**, *4*, 67-76.
- (41) Bishnoi, S.W.; Rozell, C.J.; Levin, C.S.; Gheith, M.K.; Johnson, B.R.; Johnson, D.H.; Halas, N.J *Nano Lett.* **2006**, *6*, 1687-1692.
- (42) Castro, J.L.; Lopez-Ramirez, M.R.; Arenas, J.F.; Soto, J.; Otero, J. *Langmuir* **2012**, *28*, 8926-8932.

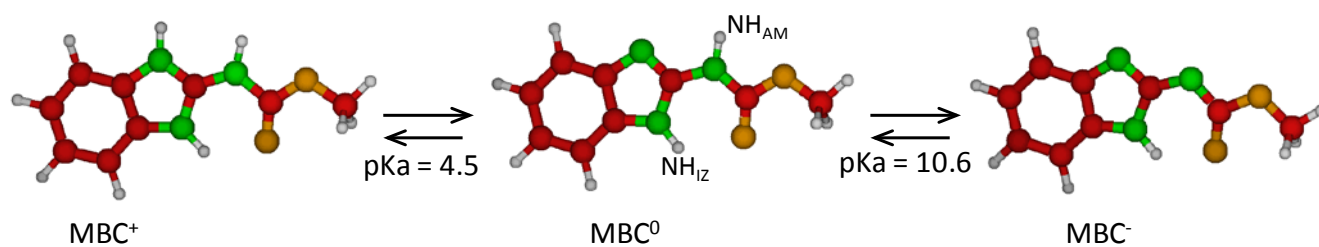


Figure 1: B3LYP/6-31G* optimized structures of different chemical species of MBC that can exist in aqueous solution depending on the pH.

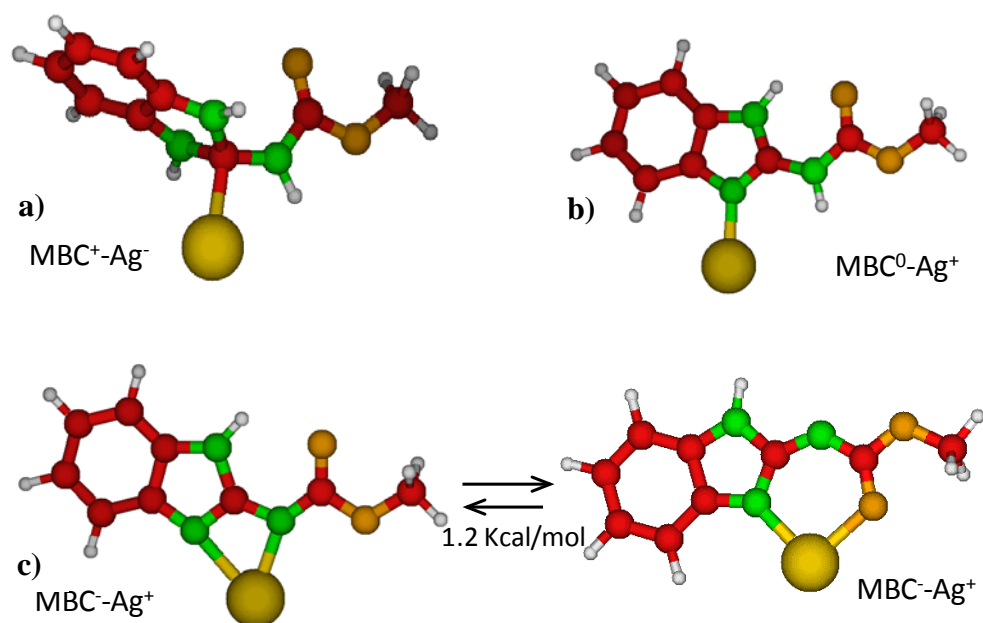


Figure 2: B3LYP/LanL2DZ optimized structures of (a) MBC^+-Ag^- , (b) MBC^0-Ag^+ and (c) MBC^--Ag^+ (Left: N-Ag-N; Right: N-Ag-O) surface complexes and energy difference between the two optimized structures of the MBC^--Ag^+ complex, being slightly more stable the complex in which the silver atom is linked to both the imidazolic nitrogen and the oxygen of the carbamate group (right).

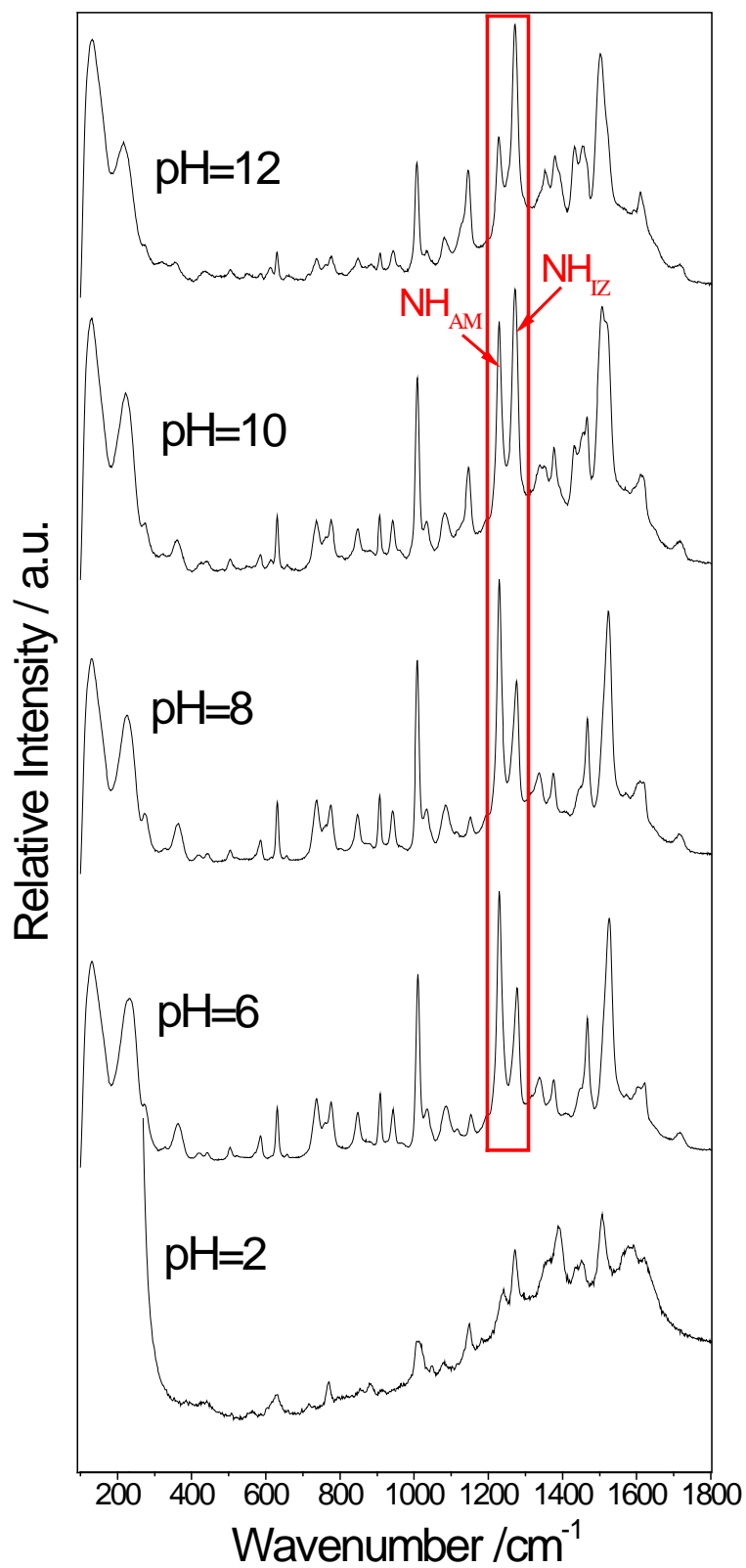


Figure 3: SERS spectra of MBC (10⁻⁵ mol/L) recorded at different pH values under 532 nm excitation.

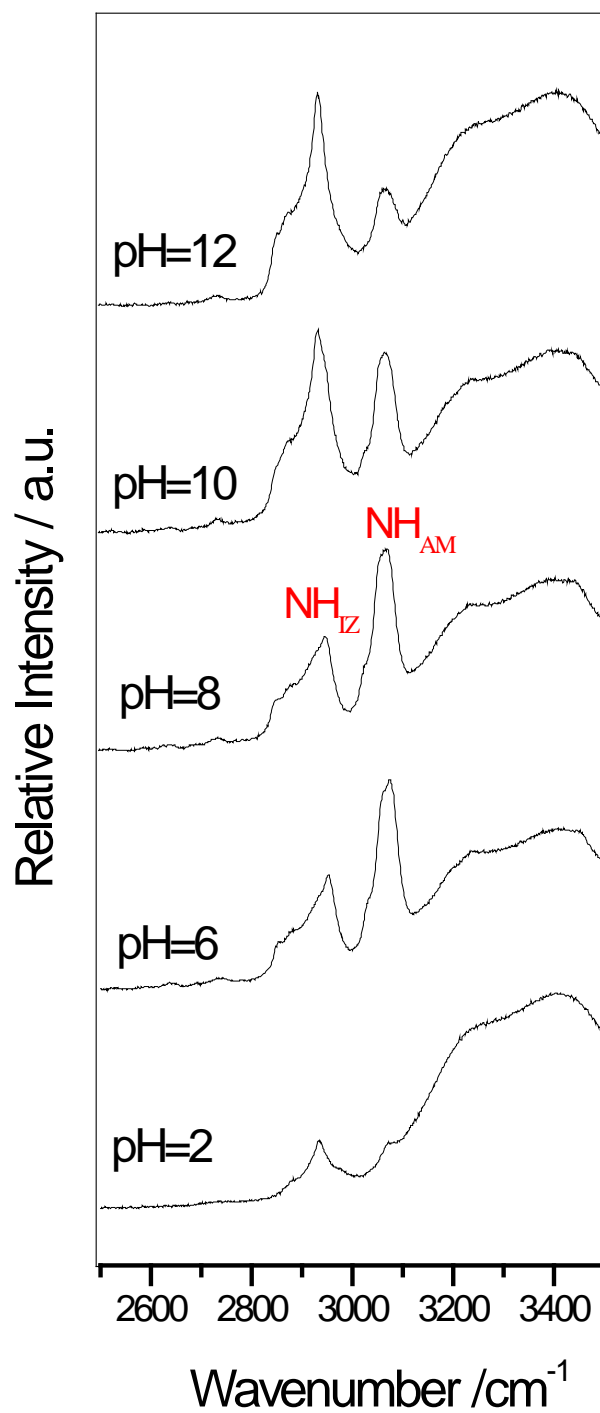


Figure 4: High wavenumber region of SERS spectra of MBC (10⁻⁵ mol/L) recorded at different pH values under 532 nm excitation.

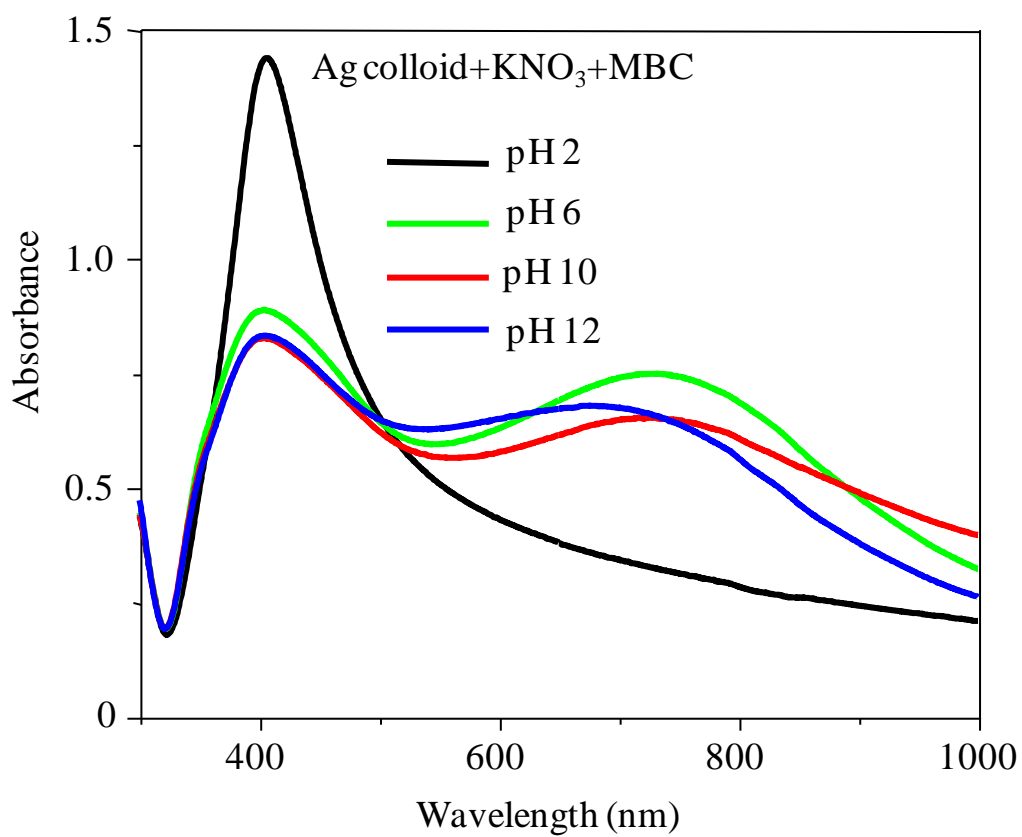


Figure 5: UV-VIS absorption spectra of Ag sols aggregated with KNO₃ and MBC at different pH values.

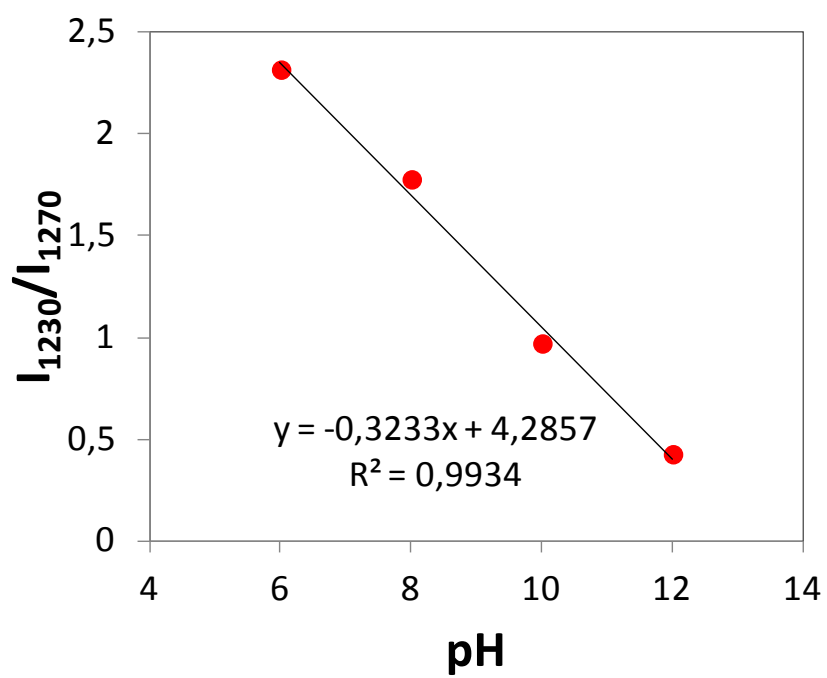


Figure 6: Dependence of the relative intensity of the SERS bands recorded at 1230 and 1270 cm^{-1} on the pH.

TOC

